Published in final edited form as:

Mol Cancer Res. 2015 March ; 13(3): 423–438. doi:10.1158/1541-7786.MCR-14-0353.

Pro-metastatic NEDD9 regulates individual cell migration via caveolin-1-dependent trafficking of integrins

Polina Y. Kozyulina[1,3], **Yuriy V. Loskutov**[2], **Varvara K. Kozyreva**[2], **Anuradha Rajulapati**[2], **Ryan J. Ice**[2], **Brandon. C. Jones**[1], and **Elena N. Pugacheva**[1,2,#]

[1]Department of Biochemistry, School of Medicine, West Virginia University Morgantown, WV, 26506, USA

[2]Mary Babb Randolph Cancer Center, School of Medicine, West Virginia University Morgantown, WV, 26506, USA

[3]Institute of Cytology Russian Academy of Sciences, St. Petersburg, Russia, 194064

Abstract

The dissemination of tumor cells relies on efficient cell adhesion and migration, which in turn depends upon endocytic trafficking of integrins. In the current work, it was found that depletion of pro-metastatic protein, NEDD9, in breast cancer (BC) cells results in a significant decrease in individual cell migration due to impaired trafficking of ligand-bound integrins. NEDD9 deficiency does not affect the expression or internalization of integrins but heightens caveolae-dependent trafficking of ligand-bound integrins to early endosomes. Increase in mobility of ligand-bound integrins is concomitant with an increase in tyrosine phosphorylation of caveolin-1 (CAV1) and volume of CAV1-vesicles. NEDD9 directly binds to CAV1 and co-localizes within CAV1 vesicles. In the absence of NEDD9, the trafficking of ligand-bound integrins from early to late endosomes is impaired, resulting in a significant decrease in degradation of ligand/integrin complexes and an increase in recycling of ligand-bound integrins from early endosomes back to the plasma membrane without ligand disengagement, thus leading to low adhesion and migration. Re-expression of NEDD9 or decrease in the amount of active, tyrosine 14 phosphorylated (Tyr14) CAV1 in NEDD9 depleted cells rescues the integrin trafficking deficiency and restores cellular adhesion and migration capacity. Collectively, these findings indicate that NEDD9 orchestrates trafficking of ligand-bound integrins through the attenuation of CAV1 activity.

[#]Corresponding author: Elena N. Pugacheva, Department of Biochemistry and Mary Babb Randolph Cancer Center, PO Box 9142, 1 Medical Center Drive, West Virginia University School of Medicine, Morgantown, WV, 26506. Phone: (304) 293-5295; Fax: (304) 293-4667; epugacheva@hsc.wvu.edu.

Disclaimers: This manuscript contains original work only and has not been published or submitted elsewhere. All of the authors have directly participated in the planning, execution and analysis of this study and have approved the submitted version of this manuscript.

Conflicts of interest:
The authors declare that there are no conflicts of interest.

Author Contributions. P.Y.K, Y.V.L., V.K.K and E.N.P conceived the project; P.Y.K and E.N.P wrote the manuscript. ECIS assays were done by P.Y.K. and Y.V.L. α/β Integrin-mediated Cell Adhesion and Millicoat ECM adhesion assays were performed by V.K.K; P.Y.K, A.R., B.J performed migration assays. All remaining experiments and data analysis were performed by P.Y.K and E.N.P.

Keywords

NEDD9; caveolin-1; integrin; endocytosis; migration

Introduction

NEDD9 is a member of the Cas family scaffolding proteins with diverse functions including regulation of the cell cycle, apoptosis, and cell motility [1, 2]. Upregulation of NEDD9 promotes epithelial to mesenchymal transition, migration, and metastasis in melanoma, glioblastoma, colon cancer and head and neck squamous carcinoma [3, 4] [5–7]. Genetic ablation of Nedd9 in a Her2-driven spontaneous mammary tumor model decreases mammary tumor incidence, initiation rate and tumor burden [8], indicating a tumor promoting role of NEDD9. The NEDD9 upregulation was detected in breast cancer (BC) patients with advanced stages, particularly in invasive and triple-negative cases [9]. NEDD9 is an integrin-signaling adaptor protein, reported to increase adhesion through activation of β1 and β3 containing integrins [2, 4]. The overexpression of NEDD9 leads to tyrosine phosphorylation of FAK and SRC kinases [10].

Caveolin-1 (CAV1) is a major component of membrane invaginations called caveolae. The caveolae serve as molecular hubs integrating adhesion signaling, through the regulation of integrin endocytosis [11]. CAV1 associates with the integrins at lipid rafts and triggers caveolin-dependent integrin internalization, thus regulating the adhesion and migration [12, 13]. Phosphorylation of CAV1 on the tyrosine 14 residue (Tyr14) triggers caveolae endocytosis and is followed by the fusion of caveolin-coated vesicles with early endosomes and integrin sorting to other endocytic compartments [14], including late endosomes/lysosomes for degradation [15–17]. The Tyr14 phosphorylation also creates a docking site for SH2 domain containing adaptor proteins, such as csk [17, 18] and NEDD9. Expression of CAV1 is associated with cancer progression and metastasis [19].

The binding of integrin receptors to the extracellular matrix (ECM) proteins promotes the assembly of cell adhesions [20]. Upon binding, integrins undergo a conformational change from inactive/bent, also called ligand-free, to an active/extended/ligand-bound conformation [21]which then transmits signals to adaptor proteins, such as NEDD9 [4, 22]. The active/ligand-bound and the inactive/ligand-free forms of integrins are internalized and trafficked through two different routes. The inactive form undergoes fast recycling between the intracellular compartment and the plasma membrane, whereas the active form of the integrin enters a slow recycling route, allowing cells to either disengage the ligand from the receptor [23] or degrade it in the lysosomes. The trafficking of the active/ECM-bound integrins to the lysosomes is considered as an alternative intracellular route used to degrade the matrix [24]. Phosphorylation of caveolin-1 on Tyr14 mediates integrin-regulated membrane domain internalization upon cell detachment [25].

In this study, we uncover a new role of NEDD9 as a regulator of integrin trafficking through CAV1-dependent endocytosis, and provide new insight into the regulation of migration of BC cells with the potential therapeutic application of anti-NEDD9 therapy for metastatic breast cancer.

Materials and Methods

Plasmids and cell culture

BT-549, ZR75-1, MDA-MB-453 (ATCC) and MDA-231-LN cells (CaliperLife Sciences) were grown based on the manufacturer's recommendations in complete medium with 10% fetal serum bovine (FBS) and infected with the GFP-expressing pGIPZ-shRNA against NEDD9 and the non-targeting scramble shRNA control in the pGIPZ vector (ThermoFisher Scientific). The cation content with the purpose of engaging or inhibiting integrins in cell culture was not manipulated. Lentiviral particles were prepared as previously described [26]. siRNAs against NEDD9 (ThermoFisher Scientific) and caveolin1 (CAV1) (Bioneer Corp.) were delivered by nucleofection (Amaxa). shRNA/siRNA sequences are available upon request. siRNAs against NEDD9 were used instead of shRNAs in some experiments where additional GFP-tagged constructs such as GFP-integrin were introduced or transient depletion was required. For the rescue experiments, mouse cDNA of Nedd9 was subcloned into pLUTZ [27]. pEGFP-caveolin-1-wt and mutant Y14F plasmids were a gift from Dr. McNiven (Mayo Clinic, Rochester, MN, USA). pFb-neo-β1-integrin-GFP plasmid was a gift from Dr. Humphries (The University of Manchester, UK).

Electric Cell-Substrate Impedance Sensing (ECIS) adhesion and migration assays

2×10^5 cells in suspension were plated on empty or coated with collagen I or matrigel 8W10E plates (Applied Biophysics) according to plate manufacturer's protocol, and electrical impedance was measured every minute for 3 or 5 hours at a frequency of 45kHz using the ECIS Applied Biophysics Morphological biosensor model 1600 (Applied Biophysics). For the migration studies, cells were plated for a 24h to form a monolayer, followed by the application of high voltage to create a wound (6V for 1min) and electrical impedance was measured every minute for 5h.

Adhesion and spreading assay

The suspension of 2×10^5 cells was plated on collagen I or matrigel coated plates, spun down to ensure even sedimentation, and bright field images were taken at indicated time points using the Leica DMIL fluorescent microscope (Leica, Microsystems Inc.). The areas occupied by individual cells were quantified using ImageJ (NIH) software.

FACS

APC- or eFluor660-conjugated antibodies against integrin β1 and β4 (eBioscience Inc.), ligand-bound integrin β1 (12G10) (EMD Millipore Corporation), ligand-free integrin β1 (mAb13) (BD Biosciences) were used according to the manufacturer's recommendations. A total of 1×10^6 cells without permeabilization were stained using the antibodies to detect surface integrins. Secondary fluorescent antibodies (BD Biosciences) were used at a concentration of 0.5 μg/L/1×10^6 cells. The APC- or eFluor660-conjugated rat or mouse isotype control (eBioscience), or nonspecific mouse or rabbit IgG were used (Sigma-Aldrich) to control for the non-specific binding.

Cell surface Biotinylation assay

Cells, pretreated with 10uM MG132, 50uM of Leupeptin (Fisher Scientific) and 0.3mMprimaquine (Sigma) where indicated, were labeled for 30min on ice with Sulfo-NHS-S-S-biotin (Thermo Fisher Sci.) in PBS; followed by incubation at 37°C to allow internalization and recycling of the labeled surface molecules for times as indicated on the figures. At each time point, the residual surface biotin was removed by 10 min incubation with 200 mM MESNA (Sigma) three times. Post-treatment cells were homogenized in PTY buffer [1] and biotinylated molecules were pulled down with streptavidin-conjugated agarose (EMD Millipore), loaded on a gel, transferred onto PVDF membrane to perform western blot analysis with anti-integrin β1 antibody.

Protein expression, western blotting, and immunoprecipitation

Western blotting was done as outlined in previous reports [1]. The primary antibodies included mouse anti-NEDD9 mAb (2G9) [1], -integrin β1, - pAP2 μ2 (Cell Signaling Technology), -integrin α1 (Abcam), -pTyr14/caveolin1, -caveolin1 (Santa Cruz Biotechnology), -GAPDH (ThermoFisher Scientific), -α-tubulin (Sigma-Aldrich), -Ras (EMD Millipore), -EGFR (eBioscience), - Transferin receptor, -adaptin-α, and -adaptin-γ (BD Bioscience). The secondary HRP-conjugated antibodies (Jackson Immuno Research Labs) were followed by using a chemiluminescent HRP Detection Reagent (Denville Scientific). The bands were digitized and quantified using a digital documentation and image analysis software (Syngene). For immunoprecipitation, the 2×10^6 cells were lysed in PTY buffer and incubated with 1μg of anti-NEDD9 mAb (2G9) or the control IgG overnight at +4°C as previously described [27].

Lipid raft purification

1.2×10^7 cells were transiently transfected with siRNAs against NEDD9 and grown to confluence. The lipid raft purification was performed according to the published protocol [28] using OptiPrep media from Axis-Shield (Dundee, Scotland).

Immunofluorescence

The cells were processed as previously described [1]. Primary antibodies include anti-pAP2 μ2, -EEA1 (Cell Signaling Technology), -clathrin light chain (BD Bioscience) and -caveolin1 (Santa Cruz). FITC-labeled bovine type I collagen (Chondrex, Inc.) was added to cells for 12–16h. Secondary antibodies included Alexa Fluor 488, 555, 647 (Life Technologies). Images were captured using the confocal microscope LSM 510 (Carl Zeiss) equipped with Photometrics QuantEM CCD camera (Photometrics), a 63X Plan Fluor, NA 1.4 objective. Images were captured every 0.35μm steps for whole cell sectioning, followed by 3D reconstruction using LSM (Zeiss) and ImageJ (NIH) software for processing and analysis. The images inside each data set were collected with the same microscopy and image capture settings, and the raw data were used for image and statistical analysis.

TIRF live cell imaging: *integrin β1 mobility assay*

The GFP-integrin β1 expressing cells were plated on delta-T4 glass bottom dishes (ThermoFisher Scientific) and imaged using a Nikon LiveScan SFC swept field inverted

microscope equipped with a perfect focus x-y stage control and z-axis motor (Nikon Inc.), a Photometrics QuantEM CCD camera (Photometrics) and a 60X Plan Fluor, NA 1.21 objective. The images were captured every 5s for 30min. NIS (Nikon) and ImageJ (NIH) software with a Mosaic particle tracker plugin was used for processing and analysis.

TIRF live cell imaging: *FITC-collagen and anti-Integrin β1-Alexa647 antibody uptake*

The cells were plated on delta-T4 glass bottom dishes (ThermoFisher Scientific), labeled with FITC- Collagen I or anti-Integrin b1-Alexa647 antibody in the presence of 0.45M sucrose. The imaging was performed as described in the integrin β1 mobility assay after triggering the label uptake by removing the sucrose.

FRAP analysis

Cells were co-transfected with the GFP-integrin β1 and siRNAs against NEDD9, plated on glass bottom dishes (InVitro Scientific), imaged with the LSM 510 (Carl Zeiss): both before photobleaching and after photobleaching of the designated area every 15 seconds for 10 minutes. The collected video sequence was analyzed using ImageJ software (NIH).

Integrin β1 trafficking assay

Cells were transfected with siRNAs against NEDD9. Anti-integrin β1 antibodies were added to the cells for 1 hour on ice and then either fixed right away or transferred to 37°C for 1 hour to internalize, stripped and recycle antibodies. The cells were then fixed with 4% PFA/PBS and processed for immunofluorescence staining. The antibodies that have been used for the recycling studies (clones 12G10 and mAb13) lock integrin receptors in their current conformation; importantly antibody binding does not change the conformation of these integrins.

Alpha/Beta Integrin-Mediated Cell Adhesion Array

The assay was performed according to manufacturer's (EMD Millipore) protocol. Multiple anti integrin subunit and integrin heterodimer specific antibodies have been used to detect changes in surface integrins, including clone P1H6 which recognizes integrin α2β1 that binds to collagen I and clone P1B5 – integrin α3β1 that binds to laminin [29]. For the detection, a GENios plate reader (Tecan) was used (detection wavelength 485/530 nm).

ECM adhesion assay

The Millicoat™ ECM Screening assay was performed according to manufacturer's (EMD Millipore Corp.) protocol. GENios plate reader (Tecan) was used (detection wavelength 540–570 nm).

Boyden chamber migration assay

Assays were carried out according to the manufacturer's protocol and as previously described [27]. Migration/invasion assays were performed using 24 well plates with BD FluoroBlok™ 8μm pore size insets (BD Biosciences). The insets were coated with 50μl of 3mg/ml matrigel for invasion assay. Cells were added to the top chamber in serum free media, 10%FBS supplemented MEM was added to the bottom chamber, and incubated for

8h. Once cells migrated through the membrane, they were labeled with CalceinAM (Life Technologies) and detected by a fluorescence plate reader (Genios) at 485/530nm excitation/emission. Top and bottom acquisitions were conducted to account for the total number of cells in the Boyden chamber insert.

Statistical Analysis

Statistical comparisons were made using Student's two-tailed t test. When more than two groups were analyzed, one-way analysis of the variance (ANOVA) was used. $P \leq 0.05$ was considered to be significant. Experimental values were reported as the means ± S.E.M. All calculations of statistical significance were performed using the GraphPad Prism package (GraphPad Software Inc., La Jolla, CA).

Results

Depletion of NEDD9 leads to adhesion and migration deficiency of breast cancer cells

NEDD9 is often upregulated in invasive, mesenchymal-like cancer cells. Nevertheless, the impact of NEDD9 expression on adhesion of breast cancer (BC) cells is unclear. To fill this gap, we depleted NEDD9 in highly invasive/migratory metastatic MDA-MB-231 and BT549 cells and assessed their adhesion and migration properties using multiple assays including *in vitro* electric cell-substrate impedance sensing (ECIS) technique [30]. For adhesion and spreading analysis, suspension of control (siCon) and NEDD9 depleted (siN2, siN3) cells were added to the ECIS chambers with the electrode at the bottom registering the current flow impeded due to adhesion/spreading of cells [31, 32]. For the ECIS wound-healing/migration assay, cells were first grown as confluent monolayers followed by application of an elevated current, which wounded the cells on the electrode, and thus caused the impedance to drop. Conversely, impedance increases, as the cells outside of the electrode migrate in to repopulate the wounded area [31, 33]. The ECIS chambers were either uncoated or coated with a thin layer of collagen I or laminin-rich matrix (matrigel) to promote adhesion. NEDD9 depletion led to a 30–40% decrease in the adhesion/spreading and migration of cancer cells (Fig.1A–G; Fig.S1A). As a complementary approach, we used Boyden chamber migration assays to evaluate changes in the migration properties of BC cells in the presence of a chemo attractant (fetal bovine serum) gradient. Similar to the ECIS assay, depletion of NEDD9 led to a significant decrease in cell migration (Fig.S1B), indicating the critical role of NEDD9 in directional migration. Overexpression of exogenous NEDD9 restored adhesion/spreading and migration proficiency of the cells (Fig.1H–J), but did not increase it above the original level, potentially due to oversaturation since MDA-MB-231 cells overexpress NEDD9 endogenously. Overexpression of NEDD9 in MDA-MB-453 and ZR75-1 BC cells with low endogenous expression of NEDD9 using a doxycycline inducible system led to a significant increase in migration (Fig.1K–L). In addition to the decrease in 2D migration, NEDD9-depleted cells exhibited up to 60% decrease in 3D migration/invasion through matrigel (Fig.S1C), confirming our previous observations [7]. The decrease in cell migration could be due to the impairment in cell adhesion to certain components of the ECM.

NEDD9 regulates adhesion of breast cancer cells to selective ECM components

Next, we determined if depletion of NEDD9 alters the binding of BC cells to different ECM proteins using the Millicoat ECM array. The array included the most abundant ECM proteins that are present under physiological conditions in the basal membrane in breast tissue, such as collagen I, IV, fibronectin and laminin [34]. We found that NEDD9 depletion lead to a significant decrease in adhesion to laminin, collagen I and IV (Fig.2A). There were no changes found in the adhesion to fibronectin or vitronectin. Additionally, to evaluate adhesion/spreading of the cells, we measured the area occupied by individual cells upon attachment to collagen I or matrigel. The depletion of NEDD9 led to a 55% decrease in adhesion to collagen I and matrigel (Fig.2B–C). These findings suggest that NEDD9 depletion may have an effect on the expression or activation of the integrin receptors responsible for binding to collagen and laminin.

NEDD9 deficiency increases the amount of integrin receptors on the cell surface

To determine if adhesion deficiency to collagen and laminin of shNEDD9 cells was caused by a decrease in the expression of certain types of integrin heterodimers, we used an alpha/beta integrin-mediated cell adhesion array to measure the total amount of individual integrins and several heterodimers (α2β1,α3β1) on the cell surface via binding to specific anti-integrin antibodies. Contrary to our expectations, the levels of the integrins: α1, α2, α4 and β1, β3, β4 and their heterodimers α2β1,α3β1were up to two-fold higher on the surface of NEDD9-depleted cells than control cells (Fig.2D–E). These findings were further confirmed by fluorescent activated cell sorting (FACS) with antibodies against β1 and β4 containing integrin heterodimers (Fig.2F, Fig.S1D). The re-expression of NEDD9 rescued this phenomenon and decreased the surface levels of integrin β1 to the control (Fig.2G). Interestingly, total protein levels of the tested integrins have not been altered upon depletion of NEDD9 (Fig.2H–K). The increase in the surface presence of certain alpha and beta integrin heterodimers correlated with the composition of the integrin receptors required for attachment to the collagen I, IV (α1β1, α2β1) and laminin (α6β1; α1β1, α2β1; α3β1; α6β4) [29]. Since the surface levels of these integrin heterodimers were increased, this suggests that NEDD9 depletion might be decreasing either the activation or the trafficking of the integrins [35].

NEDD9 deficiency heightens internalization and recycling of integrins

To determine whether NEDD9 depletion leads to internalization deficiency of integrins, we performed time course studies on the uptake of biotinylated surface molecules. Initially, the total amount of biotinylated integrin β1 on the cell surface of shNEDD9 cells was increased (Fig.S1E–F, no strip, normalized to GAPDH, confirming our FACS and IF findings (Fig.2). Internalization of biotinylated integrins was initiated by shifting the temperature to 37°C. The amount of internalized biotinylated integrin β1 was measured in cells after stripping off any surface biotin with MESNA, at the indicated time points. The amount of internalized integrins in shNEDD9 and shCon cells was similar at earlier time points (0–30 min), but shNEDD9 cells contained up to two-fold less of biotinylated integrins than the control at later time points (60 min), when normalized to the original amount of biotinylated integrins (no strip) (Fig.3A–B). The amount of intracellular biotinylated integrin depends on three

factors: a) internalization proficiency, b) intracellular degradation and c) recycling capabilities of the cells. Since proteasome and lysosome inhibitors were used during these studies, the decrease in biotinylated integrins upon NEDD9 depletion could not be attributed to the degradation of the proteins post internalization. However, this decrease could be due to the inhibition of internalization, or increased recycling of the internalized integrins back to the surface.

To discriminate between these two possibilities, we treated cells with primaquine, a drug that inhibits receptor recycling and leads to an accumulation of integrins in the endosomes, and repeated the biotinylation assay as described earlier. The siNEDD9 cells treated with the recycling inhibitor accumulated up to a two-fold more biotinylated integrin than the control cells at 60 min, when normalized to the original amount of biotinylated integrins (no strip) (Fig.3C–D), indicating that depletion of NEDD9 increased recycling of integrin receptors and potentially internalization since the amount of integrin β1 in NEDD9 depleted cells was increased upon treatment with primaquine when compared to siCon.

To visualize β1 integrin internalization, we used fluorescently labeled matrix (FITC-collagen I) and performed total internal reflection fluorescence (TIRF) live imaging analysis of internalization of integrin/ligand complexes. The collagen I binds to integrin heterodimers containing β1 integrin subunit [36], leading to the extended/ligand-bound conformation. NEDD9 depletion increased the internalization of the integrin/ligand complexes (Fig.3E). Taken together with results from the biotinylation studies, these findings indicate that NEDD9 depletion results in an increased recycling and internalization of ligand/integrin complex.

NEDD9 depletion increases mobility of integrins

To visualize β1 integrin trafficking, we used GFP-β1 integrin expressing cells and TIRF microscopy. We found that NEDD9 deficiency results in a 1.5-fold increase in mobility of β1 integrin (Fig.4A–B), as indicated by the number of GFP-β1 integrin positive foci disappearing or emerging back on the membrane in a 15 sec interval. Similarly, the fluorescence recovery after photo-bleaching (FRAP) live imaging studies of GFP-β1 integrin expressing cells showed almost two-fold increase in integrin signal recovery after photo-bleaching, indicating an increase in mobility of β1 integrin in NEDD9-depleted cells (Fig. 4C–D). To test if the exogenous expression of GFP-β1 integrin can interfere with normal integrin mobility we visualized the internalization of anti-integrin β1 antibody/integrin complex in cells expressing either empty GFP vector or GFP-β1 integrin. The rates of antibody internalization, and thus the integrin receptor, were similar in GFP-integrin and GFP-control overexpressing cells (Fig.S1G). Thus, overexpression of GFP-β1 integrin does not change the rates of integrin internalization and depletion of NEDD9 increases the trafficking of the integrins in the peri-membrane area. Next, we tested if NEDD9 depletion causes deficiency in integrin activation.

NEDD9 depletion increases the amount of integrins in the extended/ligand-bound conformation on the cell surface

To assess the activation status of the integrins, we performed FACS analysis using conformation-sensitive antibodies against extended/active/ligand-bound, (clone 12G10), and bent/inactive/ligand-free (mAb13) conformation of the β1 integrin containing receptors [37, 38]. Note, that these antibodies recognize and stabilize the specific conformation of integrins, but do not change the activation status. The decrease in NEDD9 expression resulted in up to a 50% increase in the amount of only the active form of β1 integrin on the cell surface, while there was no change in the amount of inactive form (Fig.4E), indicating that antibody binding did not artificially lead to accumulation of the stabilized isoform. The results were further confirmed by quantitative analysis of active versus inactive isoforms of β1 integrin using immunofluorescent staining (Fig.S2A–B). Upon NEDD9 overexpression in MDA-MB-453 and ZR75-1, we detected a decrease in active integrin β1 conformation compared to the control (Fig.S2C). Next, we tested whether NEDD9 depletion disrupts the binding of activated integrin β1 to its ligand, collagen I, thus decreasing adhesion and migration. Addition of FITC-collagen I to the cells showed the co-localization of labeled collagen I with active β1 integrin subunit inside and on the surface of both control and siNEDD9 cells (Fig.4F). The amount of collagen I on the surface of NEDD9 depleted cells was significantly higher than in control (indicated by white head arrows). Thus, depletion of NEDD9 does not cause a decrease in activation or binding of the β1 integrin to its ligand. Next, we tested if NEDD9 depletion leads to alterations in ligand-bound integrin trafficking.

NEDD9 deficiency increases recycling of ligand-bound integrins

To analyze the trafficking of ligand-bound and ligand-free forms, we performed a pulse-chase immunofluorescence based assay using conformation-sensitive antibodies against the β1 integrin (12G10 and mAb13) as in Fig.4, but stripped the excess of antibody from the cell surface after internalization to visualize the recycling of antibody/integrin complexes. Interestingly, after 1 hour of recycling, NEDD9 depleted cells had up to a 1.4-fold increase in the amount of active/ligand-bound integrin β1 returning to the cell surface, while recycling of the ligand-free form of the β1 integrin did not change (Fig.5A–B). Thus, NEDD9 depletion leads to an alteration in the trafficking of the ligand-bound, but not ligand-free, form of β1 integrin. Rerouting the ligand/integrin complexes might lead to inability of the ligand to disengage [23, 24] from integrin receptor. Treatment of live cells with functional antibodies (12G10 and mAb13) which recognize and stabilize the specific conformation of integrins might potentially alter the integrin conformation equilibrium; therefore we have tested the trafficking route of internalized ligand-bound and ligand-free integrins on fixed cells.

NEDD9 regulates the trafficking of ligand-bound integrins to late endosomes

The BC cells were incubated with FITC-collagen I and co-stained with conformation sensitive anti-integrin β1 antibodies (12G10) and markers of early (EEA1) and late (Rab7) endosomes (Fig.5C–D). We found that in NEDD9-depleted cells compared to control, collagen I was predominantly (70%) localized to the early endosomes and only 30% in late endosomes (Fig.5E). Similar re-distribution of active β1 integrin was observed in NEDD9

depleted cells, where majority of integrin was found in early EEA1-positive endosomes (Fig.5F, Fig.S2E). However, localization of the inactive/ligand-free β1 integrin did not change upon NEDD9 knockdown (Fig.5G, Fig.S2F). Overexpression of NEDD9 in BC cells with low endogenous NEDD9 level led to a significant shift in FITC-collagen I localization from early to late endosomes (Fig.S2D). The volume of early endosomes was substantially increased in NEDD9 deficient cells, and re-expression of NEDD9 reduced it back to control level (Fig.5H, Fig.S3A–B). Collectively, our findings indicate that regular route of recycling through the late endosomes of the ligand-bound integrins might be compromised upon NEDD9 depletion, leading to accumulation of ligand/receptor complexes in early endosomes followed by a fast recycling route back to the plasma membrane.

NEDD9 regulates caveolae-dependent trafficking of integrins through the modulation of caveolin-1 phosphorylation

Integrins are trafficked through either caveolin- or clathrin-dependent cargo systems [23, 39]. To define if late endosome trafficking deficiency in NEDD9-depleted cells is due to an altered carrier trafficking, we performed an isolation of the lipid rafts, which are known to be enriched within the caveolae [28]. In shCon and shNEDD9 cells, β1 integrin appeared in the same fractions as EGFR, CAV1 and Ras, markers of lipid rafts, but not in the fractions positive for the transferrin receptor, which is a marker of the non-raft plasma/clathrin containing membrane (Fig.6A, Fig.S3C). This observation was further confirmed by immunofluorescent staining, which revealed the co-localization of the β1 integrin with CAV1 and collagen I (Fig.6B), which was similar in siCon and siNEDD9 cells, indicating that NEDD9 depletion did not interfere with targeting of integrins to CAV1-positive compartment. Importantly, the volume of CAV1-positive endocytic vesicles was enlarged in NEDD9 deficient cells, similar to early endosomes (Fig.6C). Moreover, NEDD9 specific antibodies were able to co-immunoprecipitate the endogenous CAV1 (Fig.6D), but not AP2, a known clathrin adaptor (Fig.S3D–E). The amount of immunoprecipitated CAV1 decreased in shNEDD9 cells and the complex was absent in non-specific IgG pull-down, thus confirming the specificity of interaction. The CAV1 co-localizes with NEDD9 in some, but not all vesicles, in transiently transfected by GFP-CAV1 and RFP-NEDD9 BC cells (Fig. 6E). The active form of CAV1 identified by phosphorylation of Tyr14 was increased by up to 35% upon NEDD9 depletion (Fig.6F–G, Fig.S3F). These findings support the notion that NEDD9 is involved in the regulation of caveolae-dependent trafficking of the integrins via modulation of CAV1 phosphorylation/activation.

Depletion of caveolin-1 rescues integrin trafficking, adhesion, and migration of NEDD9 deficient cells

To test whether the increase in the amount or phosphorylation of CAV1 leads to an increase of the integrins on the cell surface, we treated NEDD9 deficient cells with siRNAs against CAV1, thus reducing the amount of total and phosphorylated CAV1. A two-fold decrease in CAV1 expression restored the levels of active/integrin β1 on the surface of the NEDD9-depleted cells to the control level (Fig. 7A–B, Panel 1). Similar results were obtained with integrin β4 (Fig.S3G). A decrease in CAV1 expression reduced the volume of the early endosomes in NEDD9-depleted cells (Fig.7C, Panel 1) and restored the migration (Fig.7D, Panel 1) and adhesion proficiency of NEDD9 depleted cells (Fig. 7E–F, Panel 1). In order to

evaluate the importance of Tyr14 phosphorylation of CAV1, we performed rescue experiments in siNEDD9+siCAV1 cells. The re-expression of the Cav1-wt, but not the Cav1-Y14F, reversed the effect of siCAV1 and recapitulated the original shNEDD9 phenotype (Fig.7A–F, Panels 2).

Thus, NEDD9 promotes BC cell adhesion and migration through regulation of CAV1-dependent integrin trafficking. The model of NEDD9's action through the inactivation of CAV1 in early endosomes and trafficking of ligand-bound integrins is outlined in Fig.7G. Additional work is needed to identify the downstream targets involved in the de-phosphorylation of CAV1 in a NEDD9-dependent manner.

Discussion

Overexpression of the NEDD9 protein is known to promote migration/invasion in multiple cancers [5, 7, 8]. We have recently reported that depletion of NEDD9 leads to a significant decrease in breast cancer metastasis due to inactivation of MMPs [7] and migration deficiency, but the molecular mechanisms of the phenomenon are not completely understood. The NEDD9-dependent migration was studied downstream of NEDD9 and its role in the upstream integrin signaling was unclear, particularly for breast cancers. To fill this gap, we used MDA-MB-231 and BT549 BC cell lines - the well characterized metastatic models of triple-negative breast cancer with high expression of NEDD9. Upon depletion of NEDD9, we observed a decrease in adhesion and migration that could be due to the decrease in expression or the activity of integrins. Surprisingly, instead of a decrease in integrin expression, NEDD9 depletion led to an increase in the amount of α1β1, α2β1 and β4 integrin heterodimers on the surface of the cells without any changes in the total protein levels. The integrin heterodimers α1β1, α2β1, and α6β4 serve as collagen and laminin receptors [40]. Nevertheless, when plated on collagen I, IV or laminin matrix, the shNEDD9 cells showed a drastic decrease in adhesion and migration compared to the control. A somewhat similar phenotype was observed in NEDD9-/- MEFs, where despite an upregulation of the α5β1 receptor, the adhesion strength to the fibronectin had been decreased compared to the control [2], but manifested with an increase in an 2D migration, suggesting that it could be cell type specific [3, 9, 22]. The matrix preferences of breast cancer cells differ from those of MEFs, and show a decreased adhesion to both fibronectin and vitronectin compared to collagens and laminin. Ahn and colleagues have shown that overexpression of NEDD9 increases, while its depletion decreases, mesenchymal MMP-dependent migration of melanoma cells in a β3-integrin/vitronectin-dependent manner [4], However, in breast cancer, the effect of NEDD9 seems to be β1/β4-integrin and therefore collagen/laminin dependent.

The ECM ligand binding stimulates the clustering and acquisition of the extended/active conformation of integrins [20]. The conformation-sensitive antibodies against the active/extended/ligand-bound (clone 12G10, binds the receptor/ligand complex rather than receptor alone) and inactive/bent/ligand-free (clone mAb13) forms of the integrin β1 have been previously tested [37, 38]. We found that NEDD9 deficiency increases the amount of active/ligand-bound β1 integrin on the surface of cells without changes in the amount of ligand-free

form. We confirmed that extended conformation corresponds to the ligand-bound form of the integrin through its engagement with fluorescently labeled matrix (collagen I).

The increase in the surface integrins could be due to the deficiency in endocytosis. Using a surface molecules biotinylation assay and live imaging, we have shown that NEDD9 depletion does not interfere with, but rather increases the uptake of integrins. The TIRF imaging and FRAP studies with the GFP-β1 integrin demonstrated up to 2.5-fold increase in the mobile fraction of the β1 integrin in the peri-membrane area of NEDD9-depleted cells. The application of the fluorescent collagen I confirmed the ability of cells to internalize the matrix with the corresponding integrin receptor upon NEDD9 depletion, arguing against the deficiency in endocytosis.

The pulse-chase antibody feeding assay using conformation-sensitive antibodies against integrin β1 indicated that NEDD9-depleted cells appeared to have up to a 30% more of antibodies on the cell's surface after recycling was initiated, suggesting that the ligand-bound integrin β1 was trafficked back to the plasma membrane without further processing and conformational changes. However treatment of live cells with antibodies which stabilize the specific conformation of integrins might potentially alter the integrin equilibrium. To address this point the trafficking route of internalized ligand-bound and ligand-free integrins were analyzed on fixed cells, leading to the similar results.

The ligand disengagement from the integrin relies on the trafficking of integrins through the endocytic compartment [41]. It is known that the ligand-bound and ligand-free β1 integrins employ different routes of trafficking [23, 42]. The endocytosis of the ligand-free β1 integrin is balanced by fast Rab4-dependent recycling from the early endosomes and targeting integrins back into the plasma membrane [43]. The ligand-bound integrins usually follow a slower Rab11/Rab25 dependent recycling route that leads the integrin/ligand complex from early endosomes to late, Rab7-positive endosomes, and lysosomes in order to degrade the ligand and recycle the free integrin back to the surface [41, 42]. NEDD9 depletion triggers an increase in mobility of integrin/ligand complex and enlargement of the CAV1/early endosome compartment, suggesting that the integrin/ligand complex is unable to enter the slow recycling loop, and after leaving early endosomes, it is targeted back to the plasma membrane instead of entering the late endosomes for processing. Immunofluorescent labeling of early and late endosomes of shNEDD9 cells incubated with FITC-collagen I demonstrated almost a two-fold decrease in the amount of active integrin β1/collagen I complexes in late endosomes. Hence, depletion of NEDD9 leads to sorting/trafficking deficiency of the ligand-bound integrins to the late endosomes.

Dysregulation of the recycling mechanism of targeting the ligand-bound integrins for degradation can reduce the cell adhesion and spreading on the matrices that are associated with the integrin dimers that undergo the recycling impairment [44]. Migration of the cells is also affected by the targeted trafficking of ligand engaged integrins to late endosomes. Ligand/integrin complexes need to be processed and recycled back to the leading edge of the migrating cell. If integrins stay locked in the extended conformation, they are transported to the rear end of the cell, thus depleting the leading edge of integrins ready to form new focal adhesions [42].

The two major routes for integrin trafficking are through the CAV1 coated caveolae and the clathrin coated pits [45]. Our data suggests that in the metastatic BC cells used in this study, the integrins are trafficked mainly through lipid rafts in a CAV1-dependent manner. Even though Arjonen and colleagues [23] showed that β1 integrin heterodimers are endocytosed through the clathrin/dynamin-dependent route, there is evidence that different dimers of β1 integrin can localize to different internalization machinery structures [46]. We have shown that the integrins co-localize with CAV1 on the cell surface as well as in the CAV1 and EEA1 positive vesicles during endocytosis. Upon NEDD9's depletion, there is a two-fold increase in the CAV1 coated vesicles and early endosomes where the internalized caveolae are supposed to fuse [14]. NEDD9 localized to internalized caveolae and binds to CAV1, but not the AP2/Cathrin complex, supporting the role of NEDD9 in the regulation of caveolin-dependent trafficking of the integrins.

It was previously shown that internalization of the caveolae was increased upon phosphorylation of CAV1 on the tyrosine 14 residue (Tyr14) [14] by focal adhesion associated kinases [17]. Both ECM-engagement of integrins [47] and cell detachment [25] stimulate Tyr14 phosphorylation of CAV1, and therefore trigger integrin-regulated membrane domain internalization. We also observed an increase in caveolin dependent ligand/integrin internalization concomitant with Tyr14 phosphorylation of CAV1 and subsequent CAV1 redisposition to the early endosomes. The depletion of CAV1 rescues the NEDD9 depletion associated phenotype by restoring migration, the amount, and the activity of the integrins on the cell's surface. To prove that NEDD9 was involved in the regulation of the caveolae-dependent trafficking via modulation of CAV1 activity, we re-expressed wild type or phospho-dead mutant of Cav1 in the siNEDD9+siCAV1 cells. The Cav1-wt, but not the phospho-dead mutant, abrogateed the rescue of NEDD9-depleted cells with siCAV1. Taken together, our findings provide new evidence that NEDD9 promotes BC cell adhesion and migration through the regulation of CAV1-dependent integrin trafficking, thus providing a new platform for the prevention of metastasis through the modulation of NEDD9.

Supplementary Material

Refer to Web version on PubMed Central for supplementary material.

Acknowledgments

We would like to thank Drs. Schaller, Grachev, Ivanov, and Mrs. Lana Yoho (West Virginia University) for providing critical feedback and editorial support during this manuscript's preparation; Dr. McNiven (Mayo Clinic) for the pEGFP-caveolin-1-wt and Y14F plasmids; Dr. Humphries (University of Manchester, UK) for the pFb-neo-GFP-β1-integrin plasmid, and Dr. Jun Liu, (West Virginia University) for CAV1 antibody; WVU Microscope Imaging Facility, supported by the Mary Babb Randolph Cancer Center and NIH grants P20 RR016440, P30 RR032138/GM103488 and S10RR026378; WVU Flow Cytometry Facility supported by NIH grants P30GM103488, P30RR032138 and RCP1101809. This work was supported by the NIH-NCI (CA148671 to E.N.P), Susan G. Komen for Cure Foundation (KG100539 to E.N.P) awards and in part by NIH/NCRR grant (5 P20 RR016440-09).

References

1. Pugacheva EN, Golemis EA. The focal adhesion scaffolding protein HEF1 regulates activation of the Aurora-A and Nek2 kinases at the centrosome. Nature cell biology. 2005; 7(10):937–946.

2. Zhong J, Baquiran JB, Bonakdar N, Lees J, Ching YW, Pugacheva E, Fabry B, O'Neill GM. NEDD9 stabilizes focal adhesions, increases binding to the extra-cellular matrix and differentially effects 2D versus 3D cell migration. PloS one. 2012; 7(4):e35058. [PubMed: 22509381]
3. Jin Y, Li F, Zheng C, Wang Y, Fang Z, Guo C, Wang X, Liu H, Deng L, Li C, et al. NEDD9 promotes lung cancer metastasis through epithelial-mesenchymal transition. International journal of cancer Journal international du cancer. 2014; 134(10):2294–2304. [PubMed: 24174333]
4. Ahn J, Sanz-Moreno V, Marshall CJ. The metastasis gene NEDD9 product acts through integrin beta3 and Src to promote mesenchymal motility and inhibit amoeboid motility. Journal of cell science. 2012; 125(7):1814–1826. [PubMed: 22328516]
5. O'Neill GM, Seo S, Serebriiskii IG, Lessin SR, Golemis EA. A new central scaffold for metastasis parsing HEF1/Cas-L/NEDD9. Cancer Res. 2007; 67(19):8975–8979. [PubMed: 17908996]
6. Singh MK, Izumchenko E, Klein-Szanto AJ, Egleston BL, Wolfson M, Golemis EA. Enhanced genetic instability and dasatinib sensitivity in mammary tumor cells lacking NEDD9. Cancer Res. 2010; 70(21):8907–8916. [PubMed: 20940402]
7. McLaughlin SL, Ice RJ, Rajulapati A, Kozyulina PY, Livengood RH, Kozyreva VK, Loskutov YV, Culp MV, Weed SA, Ivanov AV, et al. NEDD9 depletion leads to MMP14 inactivation by TIMP2 and prevents invasion and metastasis. Mol Cancer Res. 2014; 12(1):69–81. [PubMed: 24202705]
8. Izumchenko E, Singh MK, Plotnikova OV, Tikhmyanova N, Little JL, Serebriiskii IG, Seo S, Kurokawa M, Egleston BL, Klein-Szanto A, et al. NEDD9 promotes oncogenic signaling in mammary tumor development. Cancer Res. 2009; 69(18):7198–7206. [PubMed: 19738060]
9. Kong C, Wang C, Wang L, Ma M, Niu C, Sun X, Du J, Dong Z, Zhu S, Lu J, et al. NEDD9 is a positive regulator of epithelial-mesenchymal transition and promotes invasion in aggressive breast cancer. PloS one. 2011; 6(7):e22666. [PubMed: 21829474]
10. Sima N, Cheng X, Ye F, Ma D, Xie X, Lu W. The overexpression of scaffolding protein NEDD9 promotes migration and invasion in cervical cancer via tyrosine phosphorylated FAK and SRC. PloS one. 2013; 8(9):e74594. [PubMed: 24058594]
11. Patani N, Martin LA, Reis-Filho JS, Dowsett M. The role of caveolin-1 in human breast cancer. Breast Cancer Res Treat. 2012; 131(1):1–15. [PubMed: 21901387]
12. Pellinen T, Ivaska J. Integrin traffic. Journal of cell science. 2006; 119(18):3723–3731. [PubMed: 16959902]
13. Salanueva IJ, Cerezo A, Guadamillas MC, del Pozo MA. Integrin regulation of caveolin function. J Cell Mol Med. 2007; 11(5):969–980. [PubMed: 17979878]
14. Aoki T, Nomura R, Fujimoto T. Tyrosine phosphorylation of caveolin-1 in the endothelium. Exp Cell Res. 1999; 253(2):629–636. [PubMed: 10585286]
15. Irschick R, Trost T, Karp G, Hausott B, Auer M, Claus P, Klimaschewski L. Sorting of the FGF receptor 1 in a human glioma cell line. Histochem Cell Biol. 2013; 139(1):135–148. [PubMed: 22903848]
16. Schmidt-Glenewinkel H, Vacheva I, Hoeller D, Dikic I, Eils R. An ultrasensitive sorting mechanism for EGF receptor endocytosis. BMC Syst Biol. 2008; 2:32. [PubMed: 18394191]
17. Echarri A, Muriel O, Del Pozo MA. Intracellular trafficking of raft/caveolae domains insights from integrin signaling. Semin Cell Dev Biol. 2007; 18(5):627–637. [PubMed: 17904396]
18. Cao H, Courchesne WE, Mastick CC. A phosphotyrosine-dependent protein interaction screen reveals a role for phosphorylation of caveolin-1 on tyrosine 14: recruitment of C-terminal Src kinase. J Biol Chem. 2002; 277(11):8771–8774. [PubMed: 11805080]
19. Corn PG, Thompson TC. Identification of a novel prostate cancer biomarker, caveolin-1: Implications and potential clinical benefit. Cancer Manag Res. 2010; 2:111–122. [PubMed: 21188102]
20. Wehrle-Haller B. Assembly and disassembly of cell matrix adhesions. Curr Opin Cell Biol. 2012; 24(5):569–581. [PubMed: 22819514]
21. Luo BH, Carman CV, Springer TA. Structural basis of integrin regulation and signaling. Annu Rev Immunol. 2007; 25:619–647. [PubMed: 17201681]
22. Cabodi S, del Pilar Camacho-Leal M, Di Stefano P, Defilippi P. Integrin signalling adaptors not only figurants in the cancer story. Nat Rev Cancer. 2010; 10(12):858–870. [PubMed: 21102636]

23. Arjonen A, Alanko J, Veltel S, Ivaska J. Distinct recycling of active and inactive beta1 integrins. Traffic. 2012; 13(4):610–625. [PubMed: 22222055]
24. Arora PD, Manolson MF, Downey GP, Sodek J, McCulloch CA. A novel model system for characterization of phagosomal maturation, acidification, and intracellular collagen degradation in fibroblasts. J Biol Chem. 2000; 275(45):35432–35441. [PubMed: 10945978]
25. del Pozo MA, Balasubramanian N, Alderson NB, Kiosses WB, Grande-Garcia A, Anderson RG, Schwartz MA. Phospho-caveolin-1 mediates integrin-regulated membrane domain internalization. Nature cell biology. 2005; 7(9):901–908.
26. Pugacheva EN, Jablonski SA, Hartman TR, Henske EP, Golemis EA. HEF1-dependent Aurora A activation induces disassembly of the primary cilium. Cell. 2007; 129(7):1351–1363. [PubMed: 17604723]
27. Ice RJ, McLaughlin SL, Livengood RH, Culp MV, Eddy ER, Ivanov AV, Pugacheva EN. NEDD9 depletion destabilizes Aurora A kinase and heightens the efficacy of Aurora A inhibitors implications for treatment of metastatic solid tumors. Cancer Res. 2013; 73(10):3168–3180. [PubMed: 23539442]
28. Macdonald JL, Pike LJ. A simplified method for the preparation of detergent-free lipid rafts. J Lipid Res. 2005; 46(5):1061–1067. [PubMed: 15722565]
29. Carter WG, Wayner EA, Bouchard TS, Kaur P. The role of integrins alpha 2 beta 1 and alpha 3 beta 1 in cell-cell and cell-substrate adhesion of human epidermal cells. The Journal of cell biology. 1990; 110(4):1387–1404. [PubMed: 1691191]
30. Wegener J, Keese CR, Giaever I. Electric cell-substrate impedance sensing (ECIS) as a noninvasive means to monitor the kinetics of cell spreading to artificial surfaces. Exp Cell Res. 2000; 259(1):158–166. [PubMed: 10942588]
31. Chan CM, Huang JH, Chiang HS, Wu WB, Lin HH, Hong JY, Hung CF. Effects of (−)-epigallocatechin gallate on RPE cell migration and adhesion. Mol Vis. 2010; 16:586–595. [PubMed: 20376327]
32. Nethe M, Anthony EC, Fernandez-Borja M, Dee R, Geerts D, Hensbergen PJ, Deelder AM, Schmidt G, Hordijk PL. Focal-adhesion targeting links caveolin-1 to a Rac1-degradation pathway. Journal of cell science. 2010; 123(11):1948–1958. [PubMed: 20460433]
33. Gorshkova I, He D, Berdyshev E, Usatuyk P, Burns M, Kalari S, Zhao Y, Pendyala S, Garcia JG, Pyne NJ, et al. Protein kinase C-epsilon regulates sphingosine 1-phosphate-mediated migration of human lung endothelial cells through activation of phospholipase D2, protein kinase C-zeta, and Rac1. J Biol Chem. 2008; 283(17):11794–11806. [PubMed: 18296444]
34. Glukhova MA, Streuli CH. How integrins control breast biology. Current Opinion in Cell Biology. 2013; 25(5):633–641. [PubMed: 23886475]
35. Hanein D, Horwitz AR. The structure of cell-matrix adhesions the new frontier. Curr Opin Cell Biol. 2012; 24(1):134–140. [PubMed: 22196929]
36. Yamamoto M, Yamato M, Aoyagi M, Yamamoto K. Identification of integrins involved in cell adhesion to native and denatured type I collagens and the phenotypic transition of rabbit arterial smooth muscle cells. Exp Cell Res. 1995; 219(1):249–256. [PubMed: 7628540]
37. Mould AP, Akiyama SK, Humphries MJ. The inhibitory anti-beta1 integrin monoclonal antibody 13 recognizes an epitope that is attenuated by ligand occupancy. Evidence for allosteric inhibition of integrin function. J Biol Chem. 1996; 271(34):20365–20374. [PubMed: 8702772]
38. Mould AP, Garratt AN, Askari JA, Akiyama SK, Humphries MJ. Identification of a novel anti-integrin monoclonal antibody that recognises a ligand-induced binding site epitope on the beta 1 subunit. FEBS letters. 1995; 363(1–2):118–122. [PubMed: 7537221]
39. Shi F, Sottile J. Caveolin-1-dependent beta1 integrin endocytosis is a critical regulator of fibronectin turnover. Journal of cell science. 2008; 121(14):2360–2371. [PubMed: 18577581]
40. Barczyk M, Carracedo S, Gullberg D. Integrins. Cell Tissue Res. 2010; 339(1):269–280. [PubMed: 19693543]
41. Valdembri D, Serini G. Regulation of adhesion site dynamics by integrin traffic. Curr Opin Cell Biol. 2012; 24(5):582–591. [PubMed: 22981739]
42. Dozynkiewicz MA, Jamieson NB, Macpherson I, Grindlay J, van den Berghe PV, von Thun A, Morton JP, Gourley C, Timpson P, Nixon C, et al. Rab25 and CLIC3 collaborate to promote

integrin recycling from late endosomes/lysosomes and drive cancer progression. Dev Cell. 2012; 22(1):131–145. [PubMed: 22197222]

43. Bass MD, Williamson RC, Nunan RD, Humphries JD, Byron A, Morgan MR, Martin P, Humphries MJ. A syndecan-4 hair trigger initiates wound healing through caveolin- and RhoG-regulated integrin endocytosis. Dev Cell. 2011; 21(4):681–693. [PubMed: 21982645]
44. Roberts M, Barry S, Woods A, van der Sluijs P, Norman J. PDGF-regulated rab4-dependent recycling of alphavbeta3 integrin from early endosomes is necessary for cell adhesion and spreading. Curr Biol. 2001; 11(18):1392–1402. [PubMed: 11566097]
45. Margadant C, Monsuur HN, Norman JC, Sonnenberg A. Mechanisms of integrin activation and trafficking. Curr Opin Cell Biol. 2011; 23(5):607–614. [PubMed: 21924601]
46. Boyd ND, Chan BM, Petersen NO. Adaptor protein-2 exhibits alpha 1 beta 1 or alpha 6 beta 1 integrin-dependent redistribution in rhabdomyosarcoma cells. Biochemistry. 2002; 41(23):7232–7240. [PubMed: 12044154]
47. Boscher C, Nabi IR. Galectin-3- and phospho-caveolin-1-dependent outside-in integrin signaling mediates the EGF motogenic response in mammary cancer cells. Mol Biol Cell. 2013; 24(13): 2134–2145. [PubMed: 23657817]

Implications

This study provides valuable new insight into the potential therapeutic benefit of NEDD9 depletion to reduce dissemination of tumor cells and discovers a new regulatory role of NEDD9 in promoting migration through modulation of CAV1-dependent trafficking of integrins.

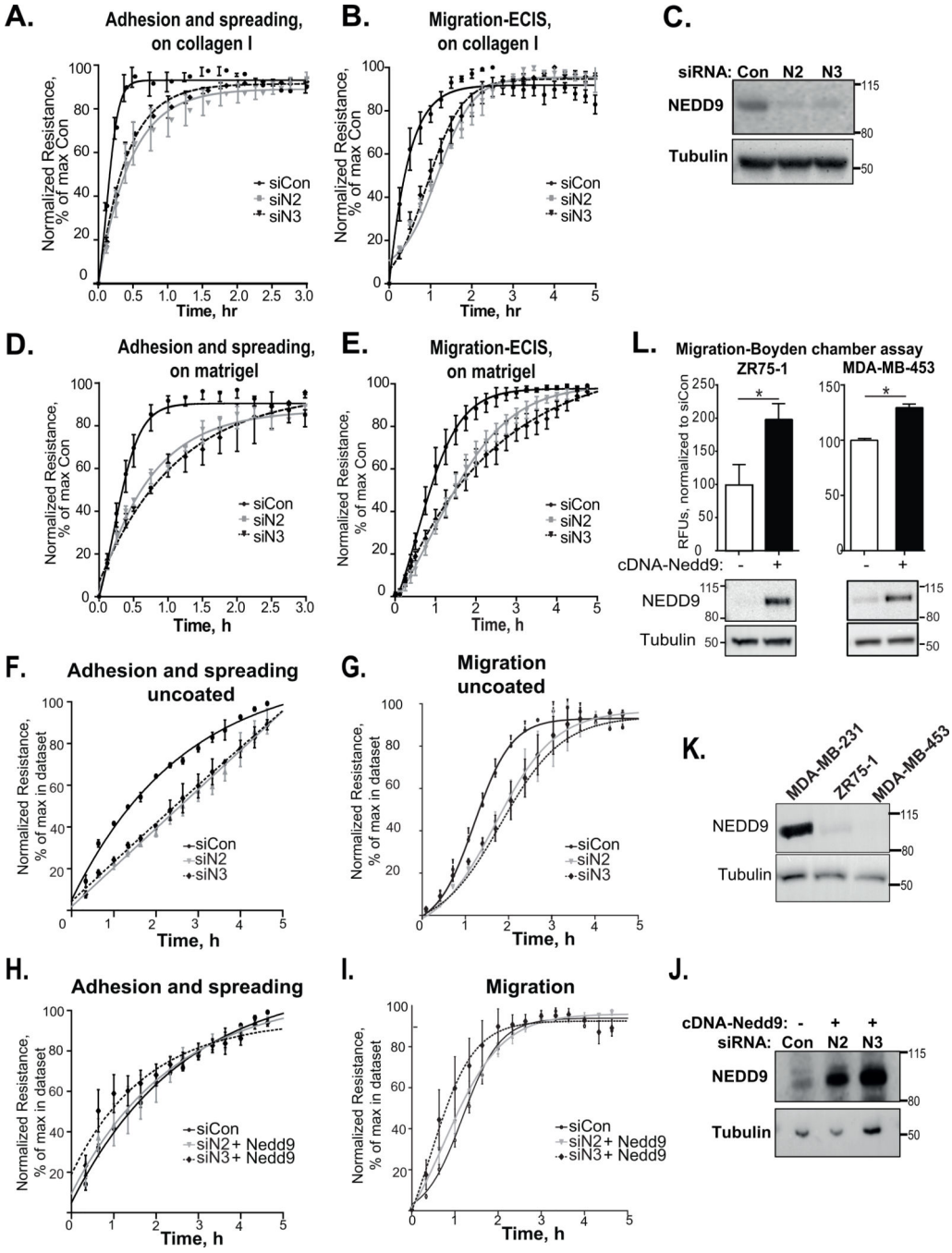

Figure 1. Depletion of NEDD9 leads to adhesion and migration deficiency of breast cancer cells

(**A–G**) ECIS-adhesion/spreading/migration assays on collagen I (A–B), matrigel (D–E) or uncoated slides (F–G). Quantification of electrical impedance during 3–5h of adhesion (A, D, F)/or migration (B, E, G) of MDA-MB-231 cells, treated with siCon or siNEDD9 (siN2, siN3); % normalized to max value in each dataset ±SEM, n=3; Adhesion: one-way ANOVA *p< 0.0001 siCon/siN2/or N3; Migration: *p< 0.037 siCon/siN2/or N3. (**C**) Western blot analysis (WB) with anti-NEDD9, -α-tubulin (loading control) antibodies. (**H–I**) similar as F–G with re-expression of cDNA-Nedd9; one-way ANOVA: p is not significant (ns). (**J**)

WB as in (H–I). (**L**) Quantification of Boyden chamber migration assay for ZR75-1 and MDA-MB-453 breast cancer cells with or without expression cDNA-Nedd9; relative intensity units (RFU) ± SEM, n=4; t-test for MDA-MB-453 *p=0.0002, for ZR75-1 *p=0.033. (**K**) Western blot analysis (WB) of NEDD9 expression in breast cancer cells (MDA-MB-231, ZR75-1, MDA-MB-453) with anti-NEDD9, -α-tubulin antibodies. (I)

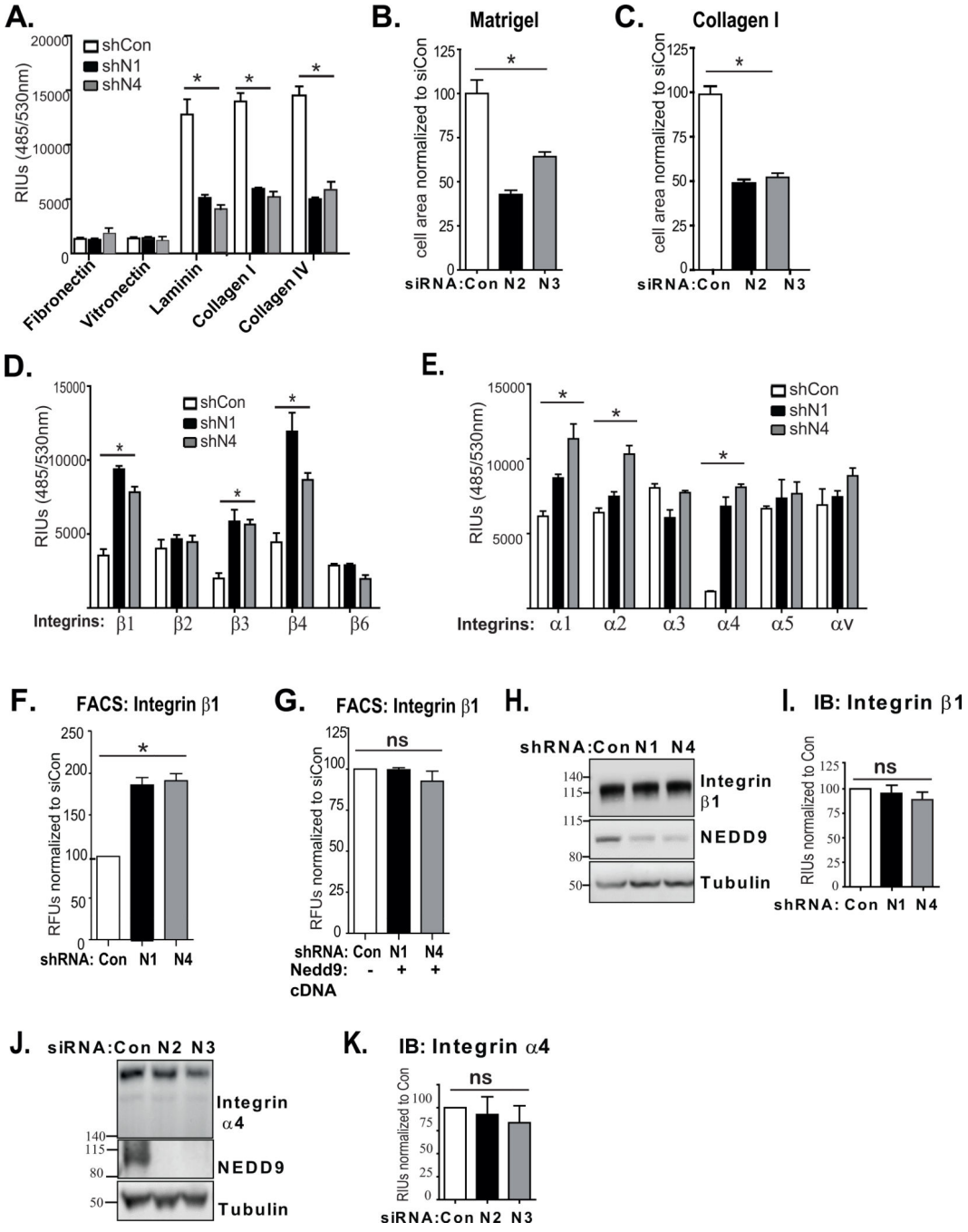

Figure 2. NEDD9 regulates adhesion proficiency of BC cells to selective ECM components and surface integrin levels

(**A**) ECM adhesion assay. Quantification of number of cells (MDA-MB-231) attached to different ECM proteins using calcein AM staining; relative intensity units (RIU) ± SEM, n=3; one-way ANOVA, shCon/shN1/or shN4: p=ns (fibronectin/vitronectin); *p= 0.0152 (laminin); *p=0.0037 (collagen I); *p=0.002 (collagen IV). (**B–C**) Adhesion and spreading assay. Quantification of individual cell area based on bright field images after 80min of incubation of cell suspension on plate coated with matrigel or collagen I; cell area

normalized to siCon ± SEM, n=50 cells; one-way ANOVA for matrigel and collagen I *p<0.0001 (**D–E**) Alpha/beta integrin array. RIU ±SEM; n=3; one-way ANOVA (shCon/shN1/or N4): *p= 0.0224 (α1); *p=0.0141 (α2); *p=0.0019 (α4); *p=0.0029 (β1); *p=0.0242 (β3); *p=0.0198 (β4). (**F**) FACS: integrin β1 surface staining in indicated cells; relative fluorescence units (RFU) %, normalized to shCon±SEM; one-way ANOVA *p<0.007 shCon/shN1 or N4 (integrin β1); (**G**) FACS as in (F) with re-expression of cDNA-Nedd9; one-way ANOVA *p=ns. (**H–I**) Left (H): WB with anti-β1 integrin and -NEDD9, -tubulin antibodies; Right (I): Quantification of WB, RIU, % to shCon±SEM; n=3; p=ns. (**J–K**) Left (J): WB with anti-α1 integrin, -NEDD9, -tubulin antibodies. Right (K): Quantification of WB, (%) of RIU to shCon±SEM; n=3; p=ns.

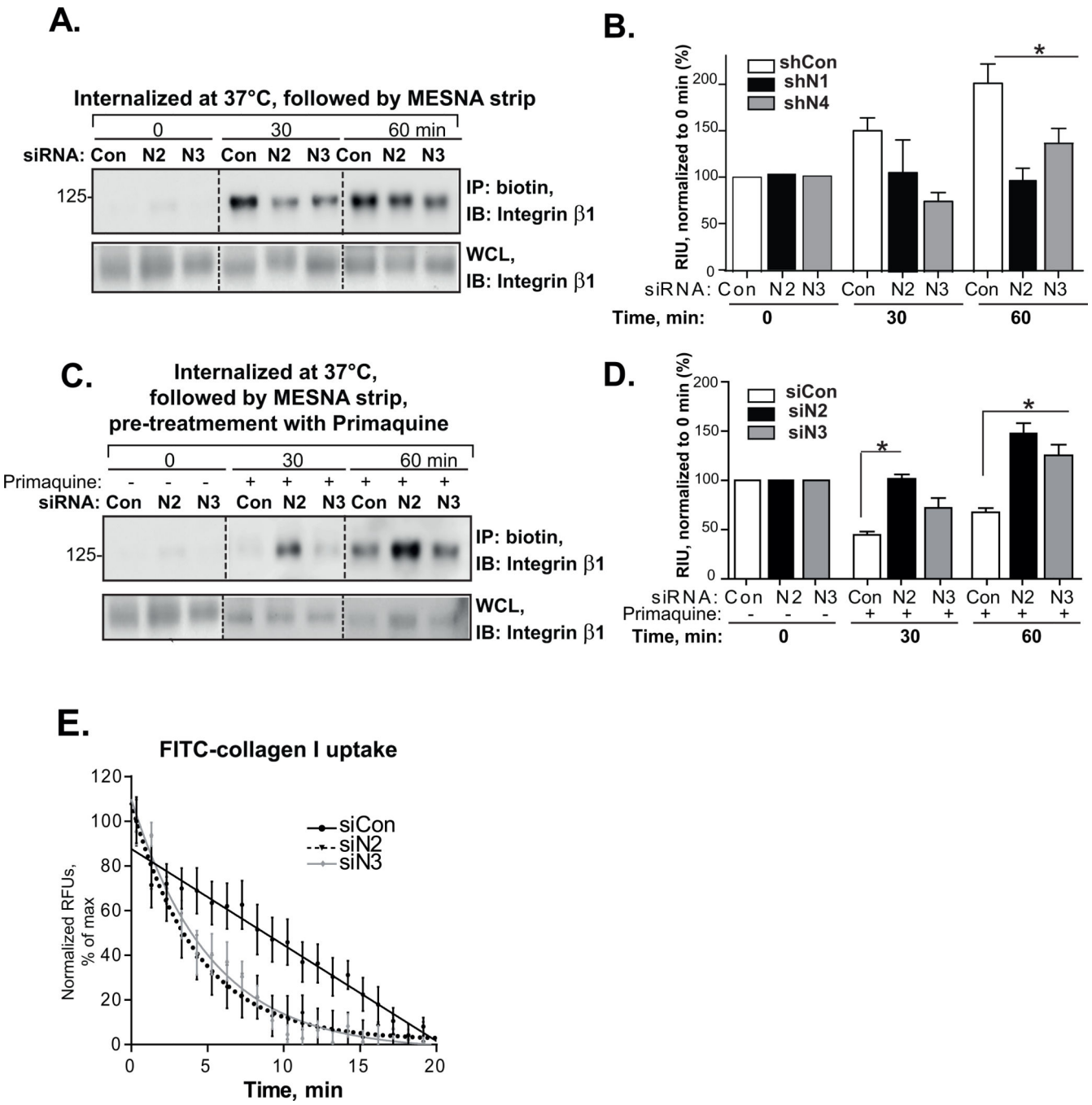

Figure 3. NEDD9 does not affect the internalization of integrins

(**A**) WB analysis with anti-integrin β1 antibodies of biotinylated integrin β1 in WCL (bottom panel) or immunoprecipitated (IP) with streptavidin agarose (top panel) from MDA-MB-231-shCon or -siN2, N3 cells. (**B**) Quantification of WB as in (A), n=3; (%) RIU to 0h conditions w/o strip (100%) ±SEM; one-way ANOVA *p< 0.0001 for shCon/shN1/or N4 at 60 min; non-significant at 30min. (**C**) WB analysis as in (A) of biotinylated integrin β1 from MDA-MB-231-siCon or -siN2, N3 cells treated with primaquine (0.3mM). (**D**) Quantification of WB as in (C), n=3; (%) RIU to 0h conditions w/o strip (100%)±SEM; one-

way ANOVA *p=0.015 for siCon/siN2, siCon/siN23 is non-significant at 30min; *p< 0.011 for siCon/siN2/or N3 at 60 min. (**E**) Quantification of FITC-collagen I uptake by MDA-MB-231-siCon, -siN2 or -siN3; normalized to maximum RFU in each data set (100%); % RFU±SEM; n=3; 10 cells/treatment; F-test for fitted lines *p <0.0001 for siCon/siN2 or siN3.

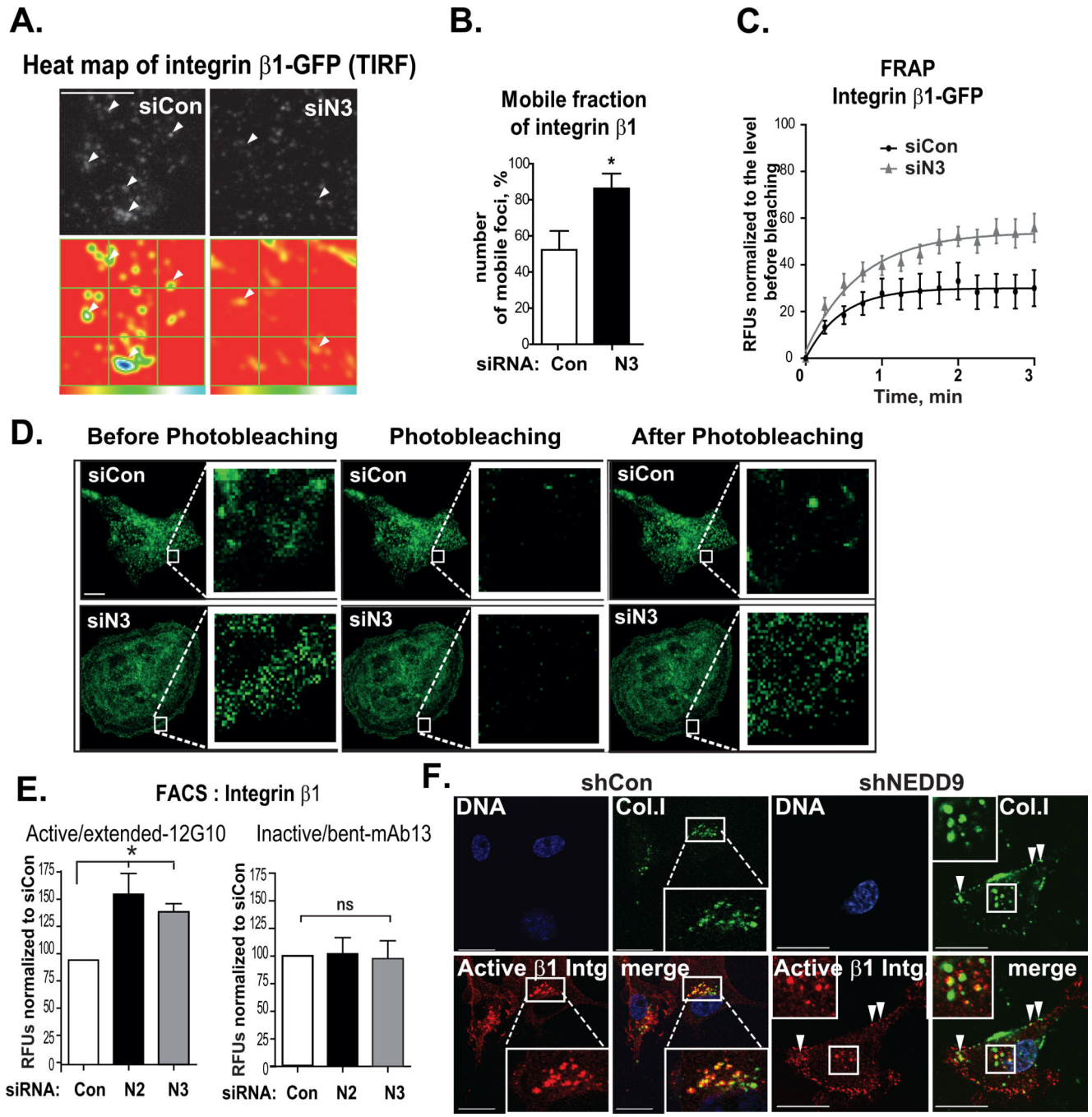

Figure 4. NEDD9 depletion increases mobility of surface integrins

(**A**) Representative heat map showing stability of β1 integrin foci, TIRF images of β1 integrin foci in MDA-MB-231-siCon, -siN3 cells, quantified 100×100 pixels frames from the movie (blue - integrin foci present on all frames of the 30 min movie, red - no GFP-integrin foci); scale bar, 10μm; white arrows-stable integrin foci. (**B**) Quantification of fraction of mobile β1 integrin foci with Mosaic plugin in ImageJ (NIH) normalized to the total number of β1 integrin foci (mobile: appearing or disappearing on the frame; and stable: persistent from frame to frame); % of mobile foci ±SEM; n=3; 5 cells/treatment; Student's t-

test *p<0.0001 for siCon/siN3. (**C–D**) Kinetics of GFP-β1-integrin fluorescent recovery after photobleaching (FRAP). (C) Quantification RFU (%) normalized to before photobleaching±SEM; n=3; 5cells/treatment; F-test performed for fitted lines, *p<0.0001 for siCon/siN3. (D) Representative confocal 3D reconstructed images as in (C) before and after (0 and 2.5 min) photobleaching; Scale bar-10μm; insets are enlarged areas of photobleaching. (**E**) FACS analysis of β1 integrin: extended/ligand-bound and bent/ligand-free conformation on the surface of MDA-MB-231-siCon, -siN2, -siN3 cells; RFU % to siCon±SEM; n=3; one-way ANOVA: *p<0.007 ligand-bound (siCon/siN2 or N3); p=ns ligand-free. (**F**) IF analysis of active β1 integrin (red) and FITC-collagenI (green) co-localization in MDA-MB-231-shCon, -shN4,) cells; 16h of treatment collagen I; DNA (blue), scale bar-20μm; inserts are the enlarged areas indicated by white rectangle, white arrows show almost complete overlap in localization of collagen I and active integrin β1.

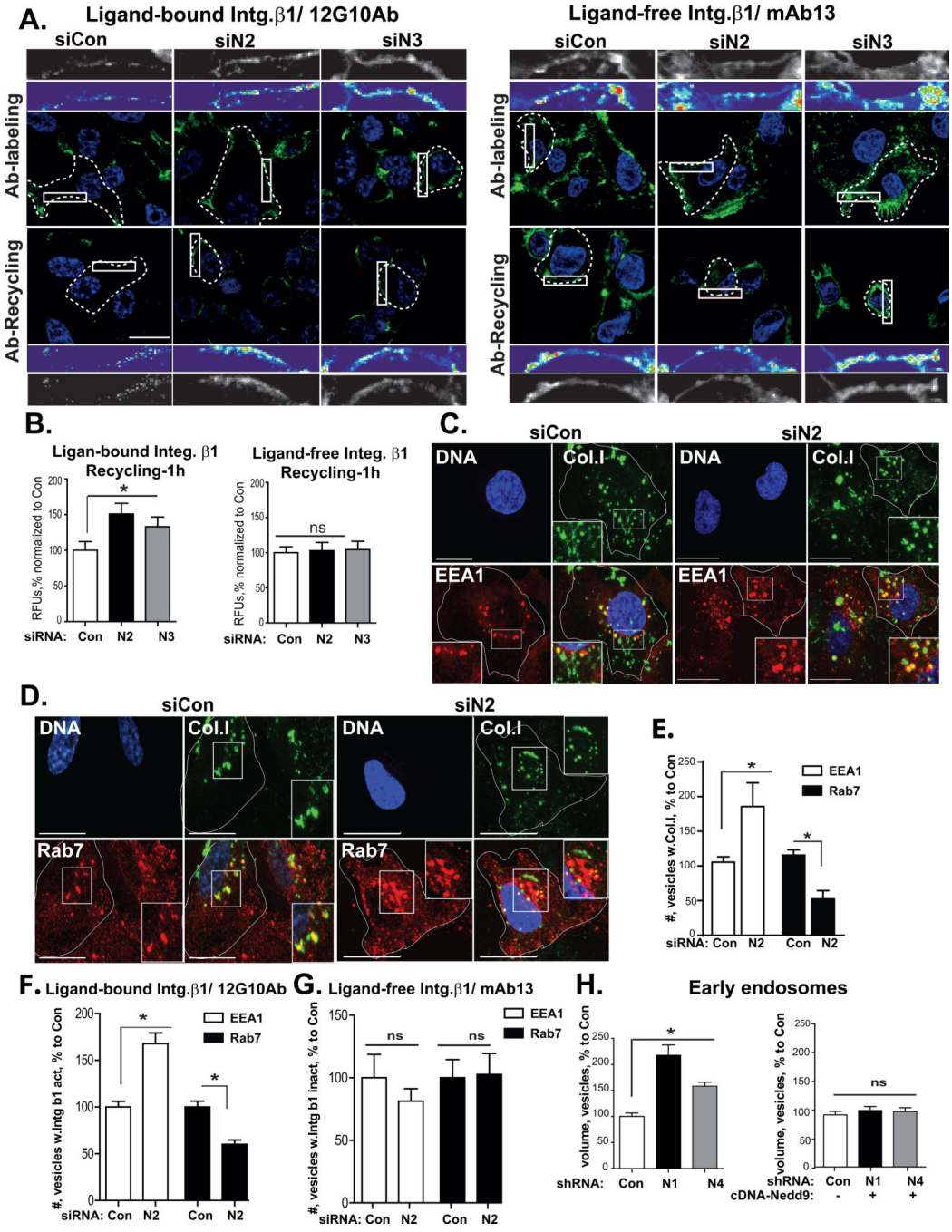

Figure 5. NEDD9 depletion increases recycling of ligand-bound integrins

(**A**) Representative confocal images of MDA-MB-231-siCon; -siN2, -siN3 cells at indicated times post surface staining with β1 integrin 12G10 and mAb13 antibodies (green), internalization, strip and 1h recycling. DNA-blue; Scale bar, 10μm; Top inserts-the enlarged areas of individual cells (dotted lines) indicated by white rectangle; middle inserts – heatmaps of fluorescent intensity of surface integrin antibody staining (12G10 and mAb13). (**B**) Quantification of the surface staining using maximum intensity projections as in (A)-1h of recycling; mean RFU, (%) normalized siCon+SEM; 30 cells/per treatment; one-way

ANOVA, 12G10: *p<0.023 (siCon/siN2/N3); mAb13: p=ns. (**C–D**) 3D reconstructed confocal images of MDA-MB-231-siCon,-siN2) cells incubated with FITC-collagen I (green) and stained with anti-EEA1 (C)/or Rab7 (D) (red), DNA (blue); Scale bar, 20μm; inserts-the enlarged areas of individual cells (white lines) indicated by rectangles in the main panel. (**E**) Quantification of number of FITC-collagen I positive vesicles (%) co-stained with EEA1 or Rab7 in cells as in (C–D), normalized to control; n=2; 15cells/per staining; t-test, EEA1: *p<0.001(siCon/siN2), Rab7: *p=0.0021 (siCon/siN2). (**F–G**) Quantification of number of integrin β1 ligand-bound (F) or ligand-free (G) positive vesicles (%) co-stained with EEA1 and Rab7 in siCon or siN2 cells, normalized to control; n=3; 15cells/per staining; t-test, EEA1: *p<0.001(siCon/siN2), Rab7: *p<0.001 (siCon/siN2). (**H**) Quantification of volume of early endosomes based on 3D reconstructed confocal images of MDA-MB-231-shCon, -shN1, -shN4) cells stained with EEA1 antibodies; cDNA-NEDD9 rescue; mean volume (%) normalized to shCon+SEM; n=3, 10 cells/treatment; one-way ANOVA: *p<0.001 for shCon/shN1 or /shN4 (EEA1); p=ns (EEA1+cDNA-Nedd9).

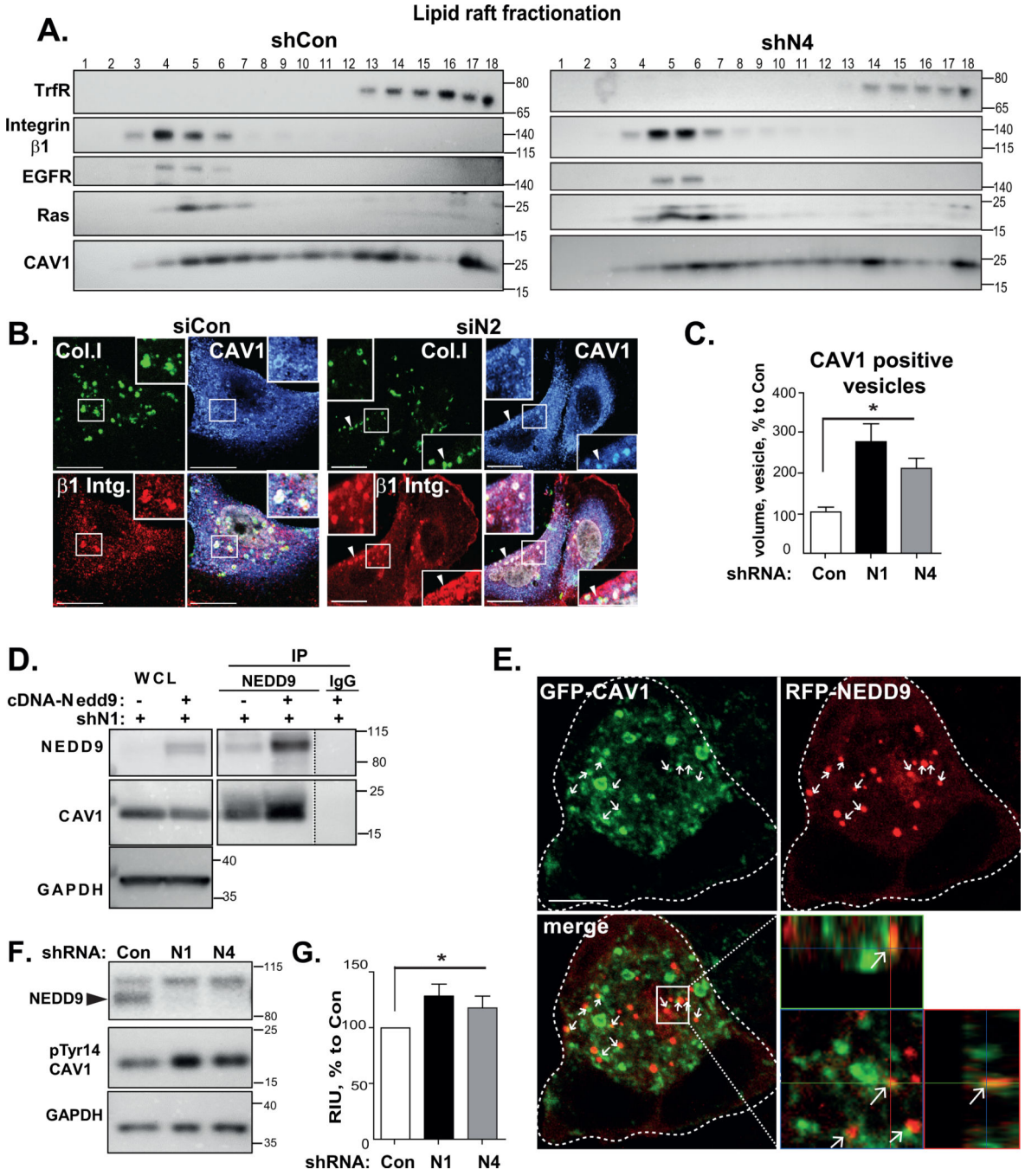

Figure 6. NEDD9 binds to and modulates activity of CAV1

(**A**) WB analysis of lipid raft fractionation, MDA-MB-231-shCon, -shN4 cells with anti-β1 integrin, -transferin receptor (TrfR), -EGFR, -Ras and CAV1 antibodies. (**B**) 3D reconstructed confocal images of MDA-MB-231-siCon, -siN2 cells; FITC-collagen I (green), β1 integrin (red), CAV1 (blue); Scale bar, 20μm; inserts-the enlarged areas of individual cells (white lines) indicated in the main panel. (**C**) Quantification of volume of CAV1-positive vesicles; MDA-MB-231-shCon and -shN1, -N4 cells based on 3D reconstructed confocal immunofluorescent images with anti-CAV1-Ab; mean volume (%)

normalized to shCon+SEM; n=3, 10 cells/treatment; one-way ANOVA: *p<0.02 for shCon/shN1 or /shN4. (**D**) WB analysis of WCL and immunoprecipitated (IP) NEDD9 with anti-NEDD9, CAV1 and GAPDH antibodies; MDA-MB-231-shN1 cells; rescue with cDNA-Nedd9, non-specific IgG – control. (**E**) Confocal images of MDA-MB-231 cells transfected with RFP-NEDD9 (red); GFP-CAV1 (green). Scale bar, 10μm; insert is the enlarged area as indicate by white rectangle; dotted lines outline cell borders; white arrows-RFP-NEDD9 co-localizes with GFP-CAV1. (**F**) WB of MDA-MB-231-shCon and -shN1,-N4 cells with anti-pTyr14-CAV1, -NEDD9 and -GAPDH antibodies. (**G**) Quantification of WBs as in (F), n=3, RIU (%) to shCon+SEM; one-way ANOVA *p<0.03 shCon/shN1/or shN4.

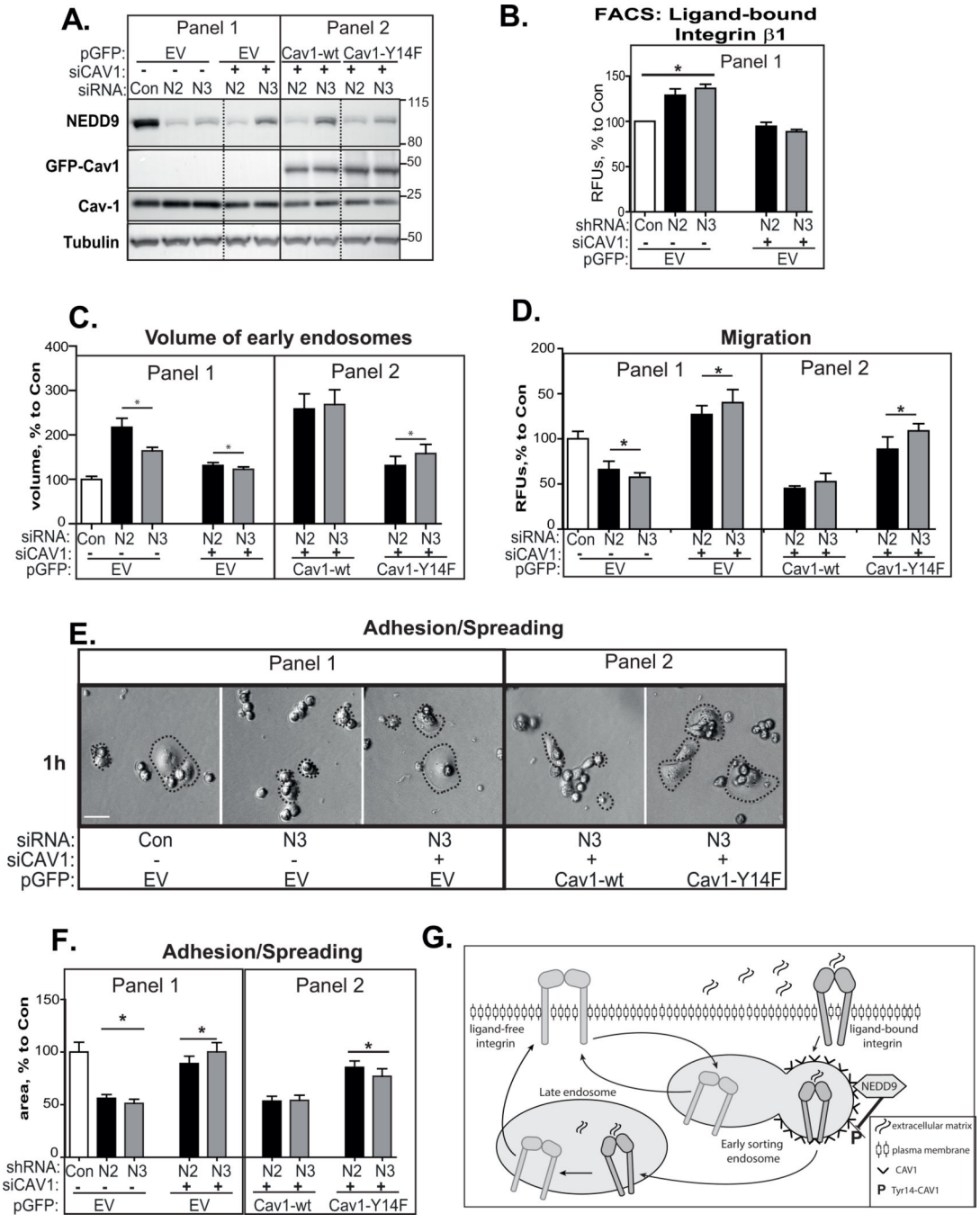

Figure 7. Depletion of CAV1 rescues integrin trafficking, adhesion and migration of NEDD9 deficient cells

(**A**) WB analysis of MDA-MB-231-siCon; -siN2, -siN3 cells treated or untreated with siCAV1 (+/−) and expressing either pGFP empty vector (EV-Panel 1), or pGFP-Cav1-wt or -Y14F (Panel 2); staining with anti-CAV1 (labeled as Cav-1 and GFP-Cav1), -NEDD9, -tubulin antibodies. (**B**) FACS of ligand-bound β1 integrin cells as in (A) Panel 1; RFU, (%) to siCon + SEM; n=3; one-way ANOVA *p<0.002 (siCon+EV/siN2–3+EV,); p=ns (siCon +EV/siCAV1+EV+siN2–3). (**C**) Quantification of volume of early endosomes in the same

cells as in (A) based on 3D reconstructed confocal images with anti-EEA1; mean volume, (%) to control + SEM; n=3; 20 cells/treatment; one-way ANOVA: *p<0.01 (siCon+EV/siN2–3+EV); p<0.0001 (siN2–3+EV/siN2–3+siCAV1+EV); p<0.02 (siN2–3+siCAV1+EV/siN2–3+siCAV1+Cav1-wt); p=ns (siN2–3+siCAV1+EV/siN2–3+siCAV1+Cav1-Y14F). (**D**) Boyden chamber migration assay. Quantification of RFU % to siCon+SEM; n=3; cells as in (A); one-way ANOVA: *p<0.003 (siCon+EV/siN2–3+EV); p<0.0001 (siN2–3+EV/siN2–3+siCAV1+EV); p=ns (siN2–3+EV/siN2–3+siCAV1+Cav1-wt); p<0.006 (siN2–3+EV/siN2–3+siCAV+Cav1-Y14F); p=ns (siN2–3+siCAV1+EV/siN2–3+siCAV1+Cav1-Y14F). (**E**) Adhesion and spreading assay; cells as in (A). Representative bright field images after 1 h of adhesion/spreading; dotted lines represent cell borders; scale bar, 10μm; (**F**) Adhesion and spreading assay. Quantification of average area of cell as in (E) % to siCon + SEM; n=3; one-way ANOVA *p<0.0001 (siCon+EV/siN2–3+EV); p<0.0001 (siN2–3+EV/siN2–3+siCAV1+EV); p=ns (siN2–3+EV/siN2–3+siCAV1+Cav1-wt); p<0.0001 (siN2–3+EV/siN2–3+siCAV+Cav1-Y14F), p=ns (siN2–3+siCAV1+EV/siN2–3+siCAV1+Cav1-Y14F). (**G**) The schematic model: The internalized through caveolae integrins delivered to early sorting endosomes; ligand-free integrins will be targeted back to plasma membrane through the fast recycling route, while ligand-bound integrins will be trafficked to late endosomes/lysosomes through the slow recycling route. NEDD9-dependent dephosphorylation of pTyr14-Cav1 is required for sorting ligand-bound integrins to late endosomes to enable disengage of integrins from ligand.